Rare Metal Materials and Engineering
Volume.50, Issue.4, April 2021
Available online at **www.rmme.ac.cn**

Science Press

Cite this article as: Dai Peng, Gao Hanfei, Wang Ning, et al. Deformation Behavior and Constitutive Modeling of Thin Pure Molybdenum Sheet at Room to Medium Temperatures[J]. Rare Metal Materials and Engineering, 2021,50(04):1156-1165.

Deformation Behavior and Constitutive Modeling of Thin Pure Molybdenum Sheet at Room to Medium Temperatures

Dai Peng[1], Gao Hanfei[2], Wang Ning[2], Fan Xiaoguang[2], Sun Mingming[1]

[1] Science and Technology on Vacuum Technology and Physics Laboratory, Lanzhou Institute of Physics, Lanzhou 730000, China; [2] State Key Laboratory of Solidification Processing, Northwestern Polytechnical University, Xi'an 710072, China

Abstract: Thin molybdenum sheet is a promising material for aerospace applications. Quantifying the mechanical behavior of the molybdenum sheet at elevated temperatures is important to understand the formability of the molybdenum component. To this end, tensile tests were carried out at different temperatures (20~500 ℃) and strain rates (5×10^{-4}~1×10^{-2} s^{-1}). The rheology, normal anisotropy and fracture behavior during tension were analyzed. The results show that the deformation resistance of thin pure molybdenum sheet is sensitive to temperature while the normal anisotropy varies little within the test temperature range. When the temperature is below 300 ℃, the strain hardening exponent increases with increasing the temperature, and it tends to be stable above 300 ℃. The elongation to fracture increases with temperature and then decreases slightly due to the dynamic strain aging. The crack is generated at the grain boundary, and the grain morphology related intergranular crack propagation causes the delamination of fractures. A modified Johnson-Cook model was established to characterize the constitutive behavior of the molybdenum sheet, of which the mean error is less than 5%.

Key words: molybdenum sheet; deformation behavior; normal anisotropy; fracture; constitutive modeling

Components in satellites and aerospace aircrafts often undergo large temperature variation in service. That may cause thermal deformation and even malfunction of the components. Thus, the molybdenum becomes an important structural or functional metallic material in aerospace due to its excellent high temperature strength and low thermal expansion. Stamping is a feasible way to manufacture thin-walled molybdenum components. However, molybdenum often exhibits poor formability at room temperature and it may require to be formed at elevated temperatures (warm plastic working). Thus, it is important to understand the correlation between the processing parameters and plastic deformation behavior of the molybdenum sheet.

By now, some work has been carried out on the variation of the plastic deformation behavior of pure molybdenum with temperature. However, most work is focused on the high temperature compression of the material, which might be used to guide the bulk forming processes[1]. Fu et al[2] carried out experimental work on the tensile properties of pure molybdenum at high temperature. They reported a rapid decrease of strength and significant increase of elongation with increasing the temperature. However, the experiments were carried out above the recrystallization temperature, which was much higher than warm forming temperature. Walde[3] investigated the plastic anisotropy of molybdenum sheets at room temperature to 100 °C. It is shown that the temperature has a strong influence on the elongation and strength but little effect on the normal anisotropy. However, the anisotropic deformation behavior above 100 °C needs further investigation. Zhang et al[4] found that the fracture mode of molybdenum sheets at room temperature was intergranular fracture. They suggested that the plastic deformation and delamination of the grains accounted for the relatively high ductility of the molybdenum plate. An in-depth investigation on the fracture mechanism was carried out by Niu et al[5] who used the in-situ scanning electron microscopy to observe the crack initiation and growth. It was confirmed that zigzag connection of the crack retarded the fracture of the specimen. However, the ef-

Received date: April 16, 2020
Corresponding author: Fan Xiaoguang, Ph. D., Professor, State Key Laboratory of Solidification Processing, School of Materials Science and Engineering, Northwestern Polytechnical University, Xi'an 710072, P. R. China, E-mail: fxg3200@126.com

fect of deformation conditions on the fracture behavior is not clear.

In this research, the deformation behavior of thin pure molybdenum sheets was investigated by tensile tests at different temperatures and strain rates. The constitutive behavior was characterized with a modified Johnson-Cook model. The results can guide the process design for warm plastic working of thin-walled molybdenum components.

1 Experiment

The as-received material was a cross-rolled pure molybdenum sheet of 0.5 mm in thickness. It was annealed at 1200 °C for 1 h to obtain a recrystallized structure, as shown in Fig.1. The curved grain boundaries suggested that a recrystallized structure without significant static coarsening was achieved. The average grain size is about 130 μm.

The tensile specimen was designed according to the ASTM E21 standard, as shown in Fig.2. The specimens were cut on plane along the rolling direction (RD). The tensile tests were carried out on the E45.105 electronic universal testing machine. The specimen was heated to the prescribed temperature at a rate of 30 °C/min, held for 20 min to impart uniform temperature distribution, and tensioned to fracture at the prescribed constraint nominal strain rate. A high temperature extensometer (3448-025M-020) was used to measure the amount of axial deformation of the gauge length.

The tensile tests were carried out at temperatures of 25, 100, 200, 300, 400 and 500 °C. The applied strain rates were 5×10^{-4}, 1×10^{-3}, 5×10^{-3}, and 1×10^{-2} s^{-1} at each deformation temperatures.

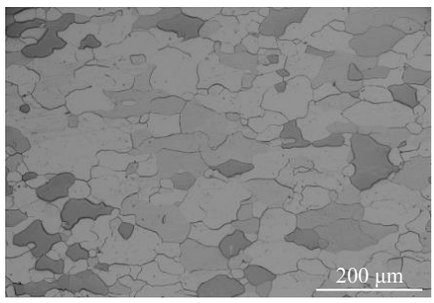

Fig.1 Microstructure of the annealed molybdenum sheet

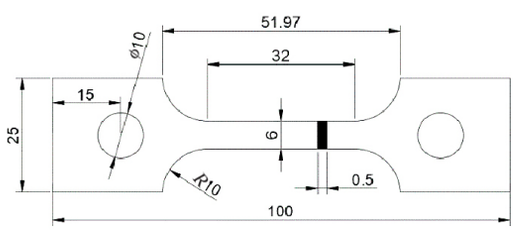

Fig.2 Specimen for the tensile test

2 Results and Discussion

2.1 Stress-strain curves

Fig.3 show the true stress-strain curves obtained by tension of the thin pure molybdenum sheets at different tempera-

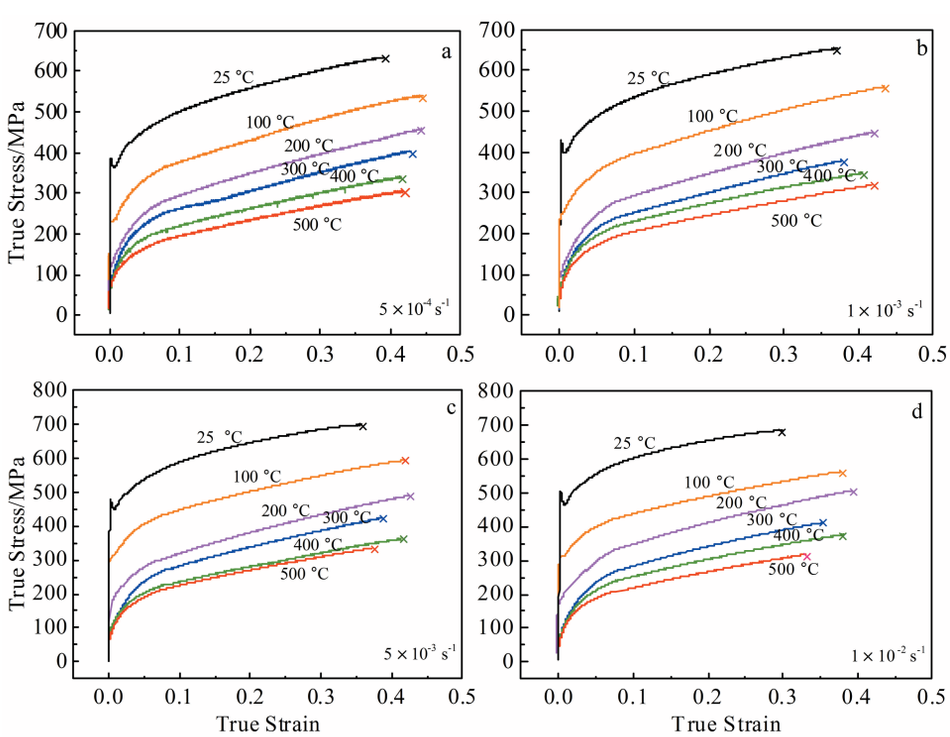

Fig.3 Stress-strain curves at different temperatures and strain rates for thin pure molybdenum: (a) $5\times10^{-4}s^{-1}$; (b) $1\times10^{-3}s^{-1}$; (c) $5\times10^{-3}s^{-1}$; (d) $1\times10^{-2}s^{-1}$

tures and strain rates. At room temperature, the molybdenum sheet exhibits a relatively high yield stress followed by a rapid yield drop at the beginning of plastic deformation. The yield drop is about 1/20 of the initial yield stress which takes place at a strain less than 0.01. Unlike the low carbon steel which exhibits a yield plateau, a rapid strain hardening is observed once the lowest yield stress is reached. Yield drop has been reported for some metallic materials with body center cubic (bcc) crystal structure, e.g., room temperature deformation of low carbon steels, β working of titanium alloys[6]. The formation of yield drop can be rationalized by the static theory and the dynamic theory[7], both involving the evolution of mobile dislocations. In the former, the unlocking of mobile dislocations from solutes results in the drop in deformation resistance. In the latter, new mobile dislocations are generated immediately and multiply rapidly after yielding, leading to significant yield drop.

The dynamic theory has been applied to the deformation of titanium alloy within the single beta phase filed. The yield drop is thought to be athermal, i.e., the extent of yield drop is not affected by the deformation temperature. Meanwhile, the coarse-grained structure restricts the mobile dislocations prior to deformation. In the current work, it is clear that the yield drop occurs at room temperature and the extent of yield drop becomes minor at 100 °C. The yield drop does not take place when the deformation temperature is above 200 °C. In addition, it seems that applied strain rate has little effect on yield drop. The extent of yield drop at room temperature increases slightly from 5.9% to 7.5% with strain rate under the current deformation conditions.

The stress-strain curves show a slight working hardening after yielding at 100 °C. When the temperature is above 200 °C, strong working hardening takes place immediately after yielding. Thus, the yield drop in current work may be rationalized by the static theory, in which the locking and unlocking of mobile dislocations play the key role. The microstructure shown in Fig.1 also suggests that there might be a sufficient number of grains within the materials as the grain coarsening is not significant.

The material undergoes significant strain hardening until fracture irrespective of temperature and strain rate. However, the deformation temperature strongly affects the yield strength (σ_s) and the ultimate tensile strength (σ_b), as shown in Fig.4. The yield stress drops dramatically with temperature below 200~300 °C but then decreases slightly. Similar behavior has been reported for pure titanium, of which the yield stress is less sensitive to temperature at 200~300 °C[8] or 350~500 °C[9]. This is often attributed to the effect of temperature on the grain boundary segregation. It is also found that the elastic modulus varies little at 300~500 °C (around 270 GPa), indicating that the variation of Peierls-Nabarro force is restricted. Thus, the yield stress is less dependent on temperature in this range. Besides, the tensile strength drops continuously with temperature. The tensile strength is mainly determined by the yield stress as well as the strain hardening during deformation, as the elongation to fracture is close at different temperatures. It is clear from Fig.3 that the strain hardening reaches the peak at 200~300 °C and then decreases with temperature. Thus, the drop of ultimate tensile strength is slower than that of yield stress below 300 °C.

It can be found in Fig.4 that both the yield stress and the tensile strength vary slightly with strain rate. The rate sensitivity is more significant at relatively low temperature (< 200 °C) but much lower above 300 °C. The decrease of rate sensitivity during warm deformation is often interpreted in terms of dynamic strain aging[8]. Dynamic strain aging often leads to a negative strain rate sensitivity parameter which seems plausible in the current work. However, when the stress-strain curves are not smoothed, some periodic yield drop at temperature of 400 °C and strain rate of 5×10^{-4} s^{-1} is actually observed, as shown in Fig. 3. Thus, dynamic strain aging may account for the low rate sensitivity at higher deformation temperatures.

2.2 Strain hardening behavior

The stress-strain curves before necking are fitted with the Swift hardening equation, and the strain hardening exponent (n) of the molybdenum sheet at different temperatures and strain rates is obtained, as shown in Fig.5. It rises linearly as temperature increases to 200~300 °C and then shows an inconspicuous variation trend. Strain hardening is often related to the slip activation. The bcc metals have as many as 48 slip systems which are more easily activated at higher temperature. Meanwhile, when the temperature is above 300 °C, the slip activation is less sensitive to temperature. This is in accordance with the fact that the measured yield stress and elastic modulus are less dependent on temperature above 300 °C.

At low temperatures, n increases with decreasing the strain rate. Meanwhile, the value scatters above 300 °C. Zhang et al[8] suggested that the low deformation temperature suppresses the dynamic recovery and the consequent softening at low strain rate. Meanwhile, the high strain rate constrains the generation and glide of dislocations and increases the flow stress, which decreases the value of n. At higher temperatures, the dynamic strain aging can improve the hardening at low temperature while the stronger dynamic recovery weakens the working hardening. Thus, it is hard to tell how the strain rate

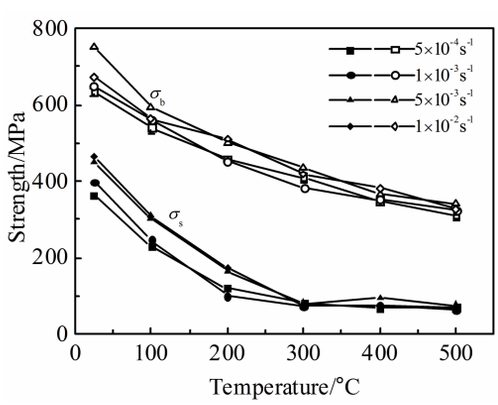

Fig.4 Variation of yield strength σ_s and tensile strength σ_b as a function of temperature and strain rate

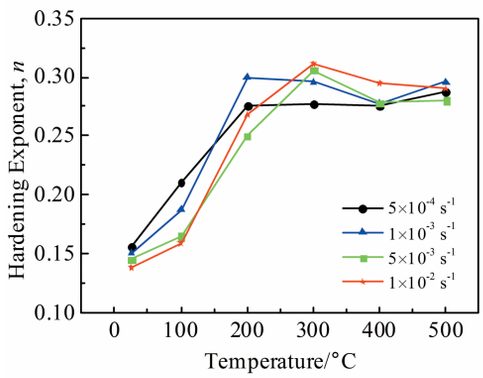

Fig.5 Strain hardening exponent as a function of temperature and strain rate

affects the strain hardening exponent at higher temperatures.

A two-segment function is used to fit the stress-strain curve, and then the variation of work hardening rate with strain and true stress is captured through calculating the first derivative of the function. The fitting results of the stress-strain curve at 25 ℃ and 1×10^{-2} s^{-1} are shown in Fig. 6d. The average *R*-square value is 0.9997. Fig.6 shows the variation of working hardening rate ($\partial\sigma/\partial\varepsilon$) with strain at different temperatures and strain rates. The molybdenum sheet shows a typical two-step working hardening. The first step involves a rapid decrease of working hardening rate with strain. The absolute value of the derivate of the working hardening rate decreases with strain. The second step is the linear decrease of working hardening rate and the slope of the curves is very small. The first step is commonly known as the stage III hardening for polycrystals[10]. The second step may correspond to the stage IV hardening[10], which depicts the constant hardening rate under large strain. It is notable that the first step of working hardening lasts for very limited strain. This may be related to the strong dynamic recovery which is associated with the bcc crystal structure of the molybdenum.

Both the first and second steps are sensitive to temperature but less affected by strain rate. At the beginning of plastic deformation, the working hardening rate increases with temperature, reaching the maximum at about 300 ℃ and then decreases with temperature. With increasing the strain, the working hardening rate drops more rapidly at higher temperatures. Meanwhile, the critical strain which separates the two steps increases with temperature. Thus, the working hardening rate is inversely proportional to temperature at the end of the first step. In the second step, it seems that the working hardening rate drops faster at low temperatures.

2.3 Normal anisotropy

As stated by Oertel et al[11], the cross rolling of molybdenum sheet often results in an incomplete α-fiber texture with rotated cube component. Such a texture often leads to strong normal anisotropy. In this work, the Lankford parameter (*r*-value) was measured to characterize the normal anisotropy. Using the specimen and experimental procedure given in Section 1, the *r*-values along different directions were measured.

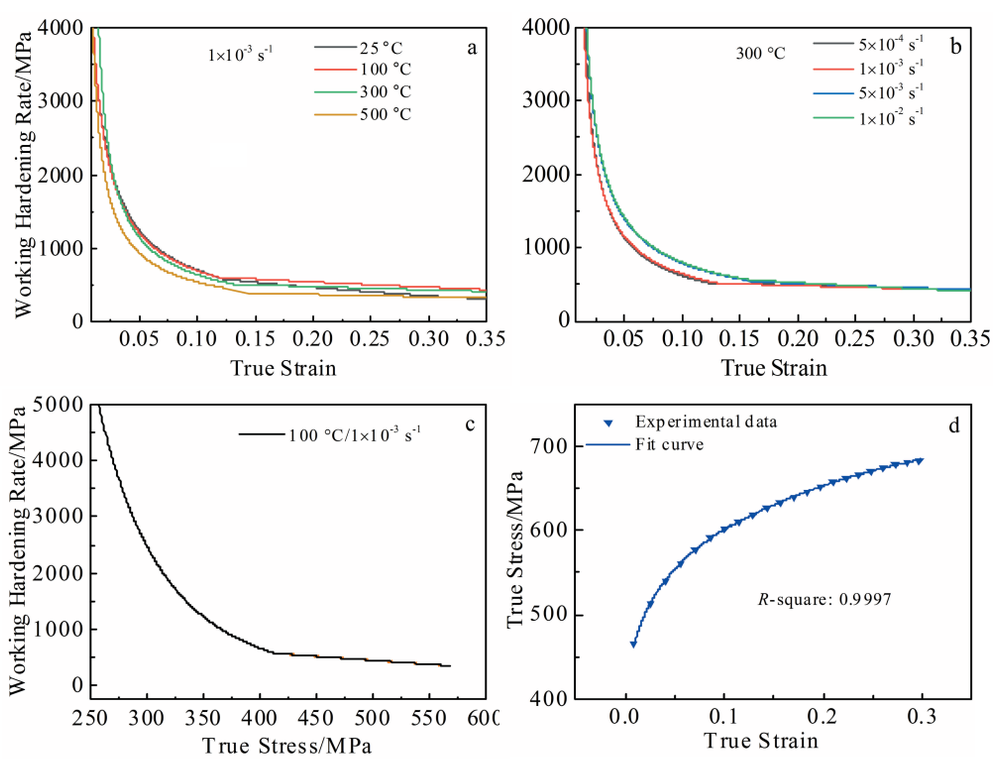

Fig.6 Variation of the work hardening rate with true strain (a, b) and true stress (c); fitting of the stress-strain curve (d)

For the un-annealed material, the measured *r*-values at room temperature are about 0.12 and 1.7 along RD and 45° direction, respectively. The value of TD is similar to that of RD. The results are close to those reported by Oertel et al[11].

The *r* value is about 0.11 along RD direction and 0.66 along 45° direction after annealing. The texture of deformed molybdenum sheet was measured by X-ray diffraction. The orientation distribution function (ODF) section of the sheet is shown in Fig.7. The results agree reasonably with Ref.[11-13], showing that rolling produces an incomplete α-fiber with peak located at the rotated cube component. Oertel et al[11] also found that the texture intensity along the γ-fiber is slightly above random after rolling. A high texture intensity on the γ-fiber can increase the *r* value significantly[14]. Annealing and recrystallization can weaken the texture intensity but do not change the texture type[11]. This may account for the low *r* value of pure molybdenum sheet after annealing. It is notable that the normal anisotropy will result in strong thickness variation during stamping, which deteriorates the formability of molybdenum sheet.

The *r* value in RD was measured at different temperatures, as shown in Fig.8. The error bar gives the variation of *r* value at different strain rates. The results suggest that the normal anisotropy varies little with temperature and strain rate. Experimental work by Walde[3] also suggest the invariance of *r* value up to 100 ℃. Thus, the deformation mode does not change within the current temperature range.

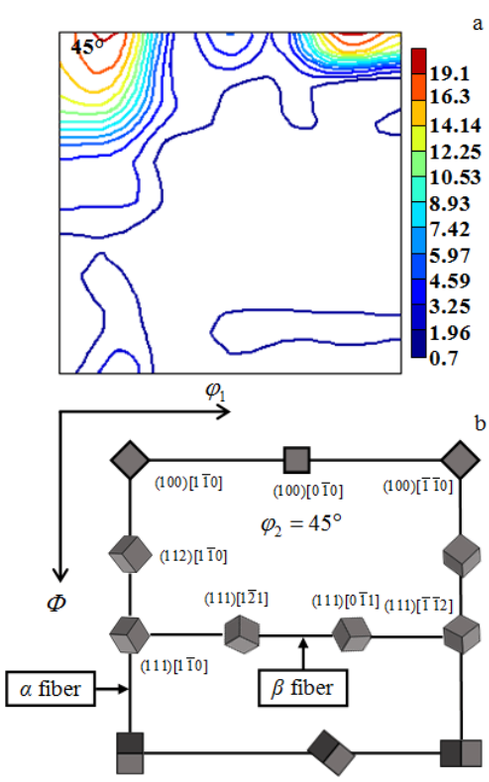

Fig.7 Measured orientation distribution function (ODF) section at φ_2= 45° of molybdenum sheet (a) and schematic showing important texture components of rolled bcc metals (b)

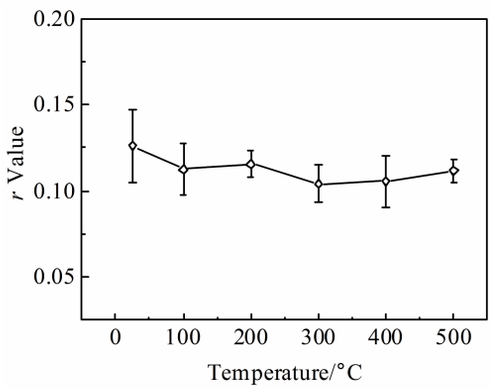

Fig.8 Measured *r* values along RD at different temperatures

2.4 Fracture behavior

Fig.9 shows the variation of elongation to fracture of molybdenum sheet at various temperatures and strain rates. The molybdenum sheet has the lowest elongation to fracture at room temperature. The elongation to fracture increases sharply with temperature, showing a peak at 100~200 ℃ and then drops slightly at 300 ℃. In most cases, the elongation to fracture fluctuates or even decreases slightly with temperature above 300 ℃.

In uniaxial tension, the specimen undergoes uniform extension until necking takes place. For the molybdenum sheet, the specimen fractures immediately once necking occurs. It can be seen in Fig.3 that the load drop is minor before necking. The micrographs of the transverse section of the necking also suggest that the length of necked region is very limited (Fig.10). The fractured specimen was pieced together and cut axially. The necked region was roughly estimated by quantify the plate thickness variation near the fracture. The measured length of the necked region is about 1 mm at 25 ℃ and 0.8 mm at 400 ℃. Thus, the elongation to fracture is determined by the uniform extension prior to necking.

The strain hardening exponent and the rate sensitivity pa-

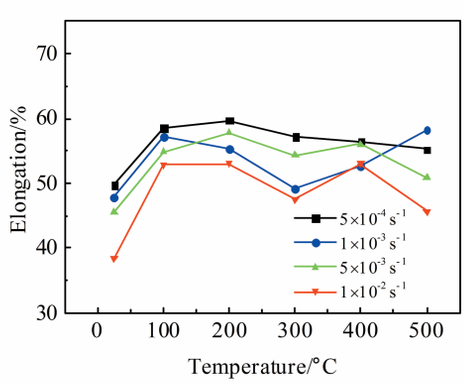

Fig.9 Variation of elongation to fracture with temperature and strain rate for molybdenum sheet

rameter are the most important indices for necking resistance. The larger the strain hardening exponent and rate sensitivity parameter, the larger the uniform extension. The strain hardening exponent increases with temperature below 200 ℃ while the rate sensitivity varies little. Thus, the elongation to fracture increases with temperature below 200 ℃. With increasing the temperature, the dynamic strain aging results in zero or negative rate sensitivity parameter. Moreover, dynamic strain aging often leads to non-uniform deformation which accelerates necking. Thus, the elongation to fracture decreases in this temperature range.

It is interesting that the tensile specimen seems to undergo a mixed mode of intergranular fracture and transgranular fracture, as shown in Fig.10 and Fig.11. Cracks form along the initial grain boundaries within the specimen at room temperature (Fig. 10b). SEM observation shows delamination of the fracture, i. e., the fracture is separated into several layers, as shown in Fig.11a. The number of the layers is 5~7. The average thickness of each layer is about 15 μm which is comparable to the grain size. Each layer has a large number of smooth surfaces which may rise from the grain boundary cracks. These surfaces tend to align with the tension axis. There are also some coarse surfaces which may result from the tearing of initial grains.

With increasing the deformation temperature, the number of the layers decreases sharply (Fig. 11b~11d). The valley in each layer becomes deeper. Moreover, the ripple pattern appears on these surfaces, indicating that additional plastic deformation may take place after the delamination of the layers. The fracture of the specimen is finally achieved via a global shear deformation, as shown in Fig.10c and 10d.

Delamination in fracture of molybdenum plate has been reported by Zhang et al[4]. It is suggested that delamination is an important cause for the high ductility of the molybdenum sheet. The rolled molybdenum sheet undergoes large thickness reduction which pancaked the grains. The secondary cracks may appear between the pancaked grains due to stress concentration, which will retard the growth of the primary cracks and release the stress concentration. Niu et al[5] reported a similar result by in-situ SEM observation.

Microstructure observation in Fig.10 suggests that the micro cracks at the grain boundaries mainly align along the tension axis within the necking region. These cracks may result from the additional tensile stress along normal direction (ND) of the sheet after necking. As the molybdenum sheet is prepared by powder metallurgy and rolling, the defects align with the normal plane. This weakens the bonding of the grains along ND. It is easy for cracks to nucleate and grow along these boundaries. When the cracks connect with each other, the delamination appears. The intergranular cracks also intersect with the intra-grain cracks. Thus, a mixture of intergranular and transgranular fracture is observed. With increasing the temperature, the stress concentration at the grain boundaries is weakened, which suppresses the nucleation of cracks at the grain boundaries. Necking results in tensile stress along the normal direction and promotes the axially intergranular crack growth. Thus, the number of the delamination decreases while some deep valleys appear on the fracture surface.

As mentioned by Zhang et al[4], the intergranular cracks may improve the ductility of the material. Free surface of the deformed specimen is smoother at high temperatures (Fig.11a and 11b), which indicates the more uniform deformation with-

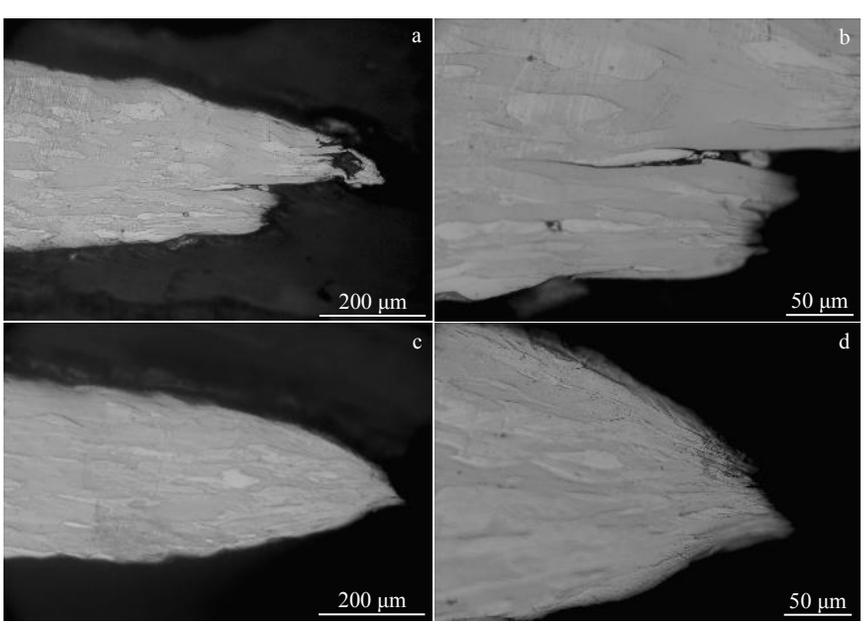

Fig.10 Low (a, c) and high (b, d) magnification optical micrographs of the transverse section of the necked region tensioned at the strain rate of 5×10^{-4} s^{-1} and temperature of 25 ℃ (a, b) and 400 ℃ (c, d) for molybdenum sheet

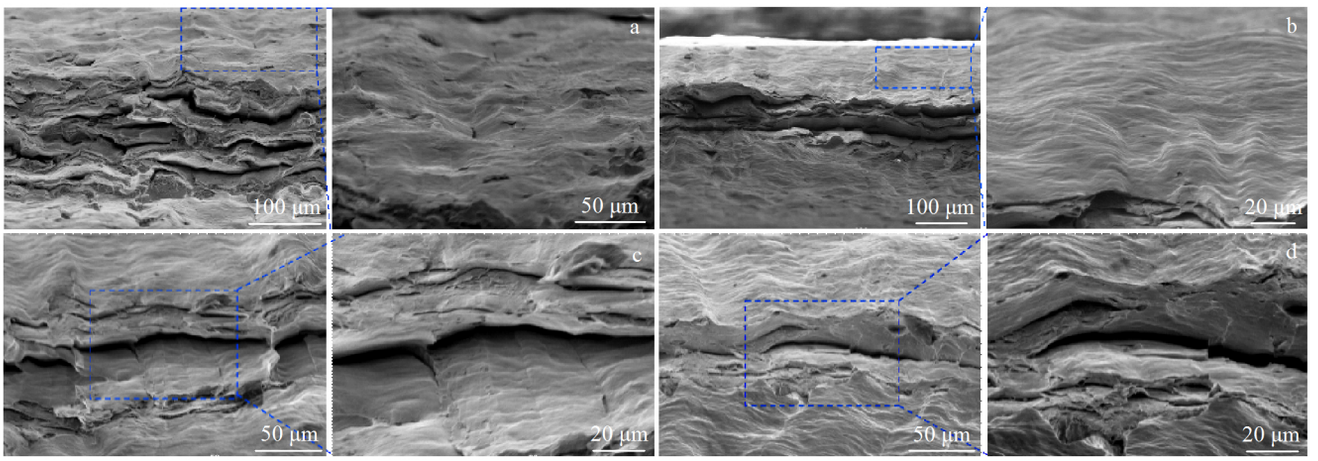

Fig.11 Fractographs of the specimen at different temperature: (a) 25 °C, (b) 200 °C, (c) 300 °C, and (d) 400 °C

in the grains. The fracture section thickness is reduced from 0.18 mm at 25 ℃ to 0.036 mm at 400 ℃ while the length of necking regions decreases from 1 mm to 0.8 mm. It indicates a rapid localization in the necking region without the restraining of intergranular cracks.

2.5 Constitutive modeling

Accurate prediction of constitutive behavior is important to the process design and optimization by numerical simulation. Among various constitutive models, the Johnson-Cook constitutive model[15] provides a simple but effective way to relate flow stress with temperature, strain and strain rate. It can predict the nonlinear stress-strain relationship under different conditions, so it is widely used in the constitutive modeling of various metallic materials[16,17]. In this research, the original Johnson-Cook constitutive model is modified to reflect the deformation behavior of the molybdenum sheet. The Johnson-Cook constitutive model in the original form is expressed as follows:

$$\sigma = (A + B\varepsilon^n)(1 + C\ln\frac{\dot{\varepsilon}}{\dot{\varepsilon}_0})(1-T^{*m}) \quad (1)$$

where σ is flow stress, ε is plastic strain, $\dot{\varepsilon}$ is strain rate, and $\dot{\varepsilon}_0$ is the reference strain rate (1×10^{-3} s^{-1} in this study). The value of the reference strain rate lies within the range of the applied strain rate. The applied strain rate is normalized to a value around 1, which makes the parameter identification easier. $T^*=(T-T_r)/(T_m-T_r)$ is a normalized temperature, where T is the deformation temperature, T_r is the reference temperature (25 ℃ in this study) and T_m is the melting point of the material (2610 ℃ in this study). A, B, C, n, and m are the fitting parameters. A denotes the flow stress at the reference temperature and strain rate. The three terms on the right describe the effect of strain hardening, strain rate hardening and thermal softening on deformation resistance.

In the current work, the strain hardening behavior of pure molybdenum sheet shows strong non-linearity with deformation temperature and strain rate, as illustrated in Fig. 3. The original form of Johnson-Cook model cannot describe this phenomenon. It has been improved to enhance the prediction accuracy[18-22]. Zhang et al [22] modified the model to take the coupling effect of strain and temperature into consideration, which may be more appropriate for the present work. The improved Johnson-Cook model proposed by Zhang et al[22] is given as follows:

$$\sigma = [A(1-T^{*m}) + B(T^*)\varepsilon^n](1 + C\ln\frac{\dot{\varepsilon}}{\dot{\varepsilon}_0}) \quad (2)$$

where $B(T^*)$ is a function of T^*. The parameters in Eq.(2) are determined by the following procedure.

(1) A and n

When $T=T_r$ and $\dot{\varepsilon}=\dot{\varepsilon}_0$, Eq.(2) is simplified as:

$$\sigma=A+B(T^*)\varepsilon^n \quad (3)$$

When $\varepsilon=0$, $A=\sigma_{0.2r}$ ($\sigma_{0.2r}$ is the yield stress at reference temperature and strain rate), taking the logarithm on the two sides of Eq.(3), it comes:

$$\ln(\sigma-A)=\ln(B(T^*))+n\ln\varepsilon \quad (4)$$

where $B(T^*)$ is a constant at a given temperature and n is the slope of the $\ln(\sigma - A)$-$\ln\varepsilon$ curve.

(2) C

When $T=T_r$ and $\varepsilon=0$, Eq.(2) is simplified as:

$$\sigma_{0.2} = A(1 + C\ln\frac{\dot{\varepsilon}}{\dot{\varepsilon}_0}) = \sigma_{0.2r}(1 + C\ln\frac{\dot{\varepsilon}}{\dot{\varepsilon}_0}) \quad (5)$$

C is the slope of the $(\sigma_{0.2}/\sigma_{0.2r}-1)$ - $\ln\dot{\varepsilon}/\dot{\varepsilon}_0$ curve.

(3) m

When $\dot{\varepsilon} = \dot{\varepsilon}_0$ and $\varepsilon=0$, Eq.(2) is simplified as:

$$\sigma_{0.2} = A(1-T^{*m}) = \sigma_{0.2r}(1-T^{*m}) \quad (6)$$

Taking the logarithm on both sides of Eq.(6), it comes:

$$\ln(1-\frac{\sigma_{0.2}}{\sigma_{0.2r}}) = m\ln T^* \quad (7)$$

Thus, m is the slope of the $\ln(1 - \sigma_{0.2}/\sigma_{0.2r})$ - $\ln T^*$ curve.

(4) Function $B(T^*)$

When $\varepsilon = \varepsilon_b$ (where ε_b is the strain at fracture point), tensile strength (σ_b) is reached, and Eq.(2) can be simplified as:

$$\sigma_b=A(1-T^{*m})+B(T^*)\varepsilon_b^n \quad (8)$$

Combined with Eq.(6), $B(T^*)$ can be determined by:

$$B(T^*)=\frac{\sigma_b-\sigma_{0.2}}{\varepsilon_b^n} \quad (9)$$

σ_b and ε_b^n can be expressed as a function of temperature:

$$\sigma_b=\sigma_{br}(1-T^{*m_b}) \quad (10)$$

$$\varepsilon_b = \varepsilon_{br}(1 + P_1T^* - P_2T^{*P_3}) \quad (11)$$

where σ_{br} and ε_{br} are the fracture stress and strain at break at reference temperature and strain rate, respectively, when m_b, P_1, P_2, and P_3 are constants.

Table 1 gives the model parameters obtained from the experimental data of the molybdenum sheets. Fig. 12 compares the predicted flow stress by the above model and the experimental results. It is clear that the above model fails to predict deformation behavior of the molybdenum sheet. Therefore, the model needs to be modified to improve its accuracy.

The m value in the above model is taken as the slope of the $\ln(1-\sigma_{0.2}/\sigma_{0.2r})$ - $\ln T^*$ curve shown in Fig.13. The value of m should be different under different temperature conditions. Such an assumption will deteriorate the accuracy of the model. Therefore, it is necessary to correct the form of m. Assuming m is a function of T^* which takes the following form:

$m=a_1+b_1T^*+c_1T^{*2}+d_1T^{*3}$, Eq.(7) can be rewritten as:

$$\ln\left(1-\frac{\sigma_{0.2}}{\sigma_{0.2r}}\right) = (a_1 + b_1T^* + c_1T^{*2} + d_1T^{*3})\ln T^* \quad (12)$$

When $\dot{\varepsilon} = \dot{\varepsilon}_0$ and ε=0, the $\ln(1-\sigma_{0.2}/\sigma_{0.2r})$ - $\ln T^*$ curve is fitted by Eq.(12) and the parameters a_1, b_1, c_1, and d_1 can be obtained. The results are shown in Fig.14.

Similarly, m_b is assumed to be a function of T^* given by $m_b=a_2+b_2T^*+c_2T^{*2}+d_2T^{*3}$. The parameters a_2, b_2, c_2, and d_2 can be obtained by the same method. In order to describe the effect of temperature on the stress and strain at the fracture, a quadratic term, $\varepsilon_b=\varepsilon_{br}(1+P_1T^*+P_2T^{*2}-P_3T^{*P_4})$, is added to the expression of ε_b. Using this equation to fit the ε_b - T^* curve, the parameters P_1, P_2, P_3, and P_4 can be obtained. The parameters of the modified Johnson-Cook model are shown in Table 2.

Model predictions are shown in Fig. 15. It can be seen that the prediction results at different temperatures and strain rates agree well with the experimental results. The average relative error is less than 5% within the test temperature and strain rate range.

It can be seen that the predicted results agree well with the experiment below 200 ℃. When the temperature is above 200 ℃, there are some discrepancies at plastic strain below 0.2 (Fig.15a and 15b). This is because the modified Johnson-Cook model predicts the stress-strain relationship by using the yield point and tensile strength point of the experimental results as reference points. It can reflect the variation trend of material hardening behavior with temperature on the whole, but cannot reflect the change of hardening mode in the initial

Table 1 Material parameters for the modified Johnson-Cook model by Zhang et al[22]

A	n	C	m	m_b	P_1	P_2	P_3
397.76	0.5032	0.0857	0.4226	0.6956	3726.7	3728.7	1.0000

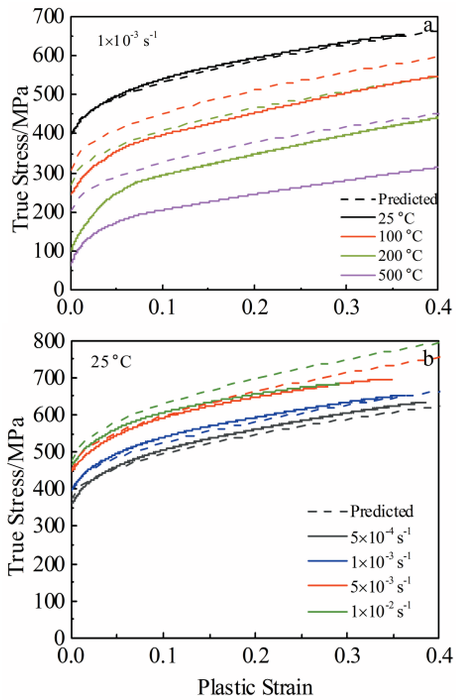

Fig.12 Comparison between predicted flow stress by Zhang's model and measured flow stress at different temperatures and strain rates: (a) $\dot{\varepsilon}$=1×10^{-3} s^{-1} and (b) 25 ℃

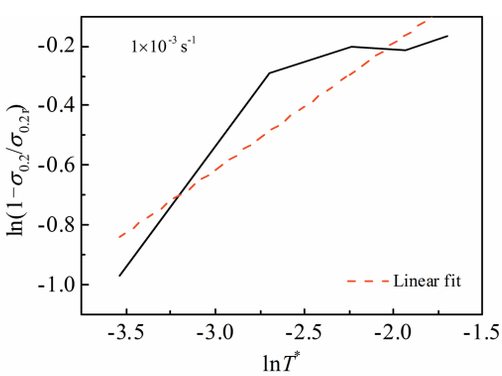

Fig.13 $\ln(1-\sigma_{0.2}/\sigma_{0.2r})$ - $\ln T^*$ curves

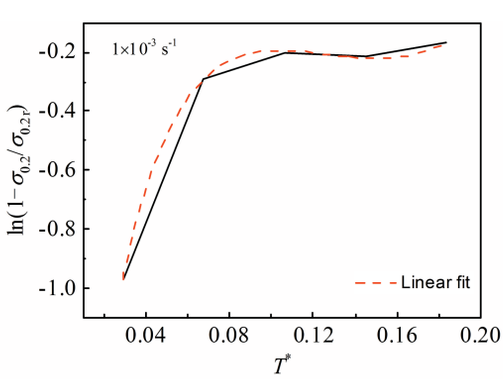

Fig.14 $\ln(1-\sigma_{0.2}/\sigma_{0.2r})$ - T^* curves

Table 2 Parameters for the modified Johnson-Cook model

Material parameters	Value	Material parameters	Value
A	397.8	b_2	-7.200
n	0.6366	c_2	50.97
C	0	d_2	-116.0
a_1	0.5458	P_1	127.8
b_1	-12.12	P_2	45.14
c_1	101.7	P_3	147.3
d_1	-266.5	P_4	1.049
a_2	0.7179		

plastic strain stage. However, when the strain is lower than 0.2, the hardening behavior of pure molybdenum sheet above 200 ℃ changes significantly. As shown in Fig. 5, n increases linearly with temperature to 200~300 ℃ and then varies little. This makes the hardening behavior change significantly with increasing the temperature. The bcc metals have as many as 48 slip systems which are more easily activated at higher temperatures. Meanwhile, when the temperature is above 300 ℃, the slip activation is less sensitive to temperature, which leads to changes of the hardening behavior. Therefore, the model has a more obvious error in the prediction of the initial stage of the stress-strain curve under higher temperature conditions.

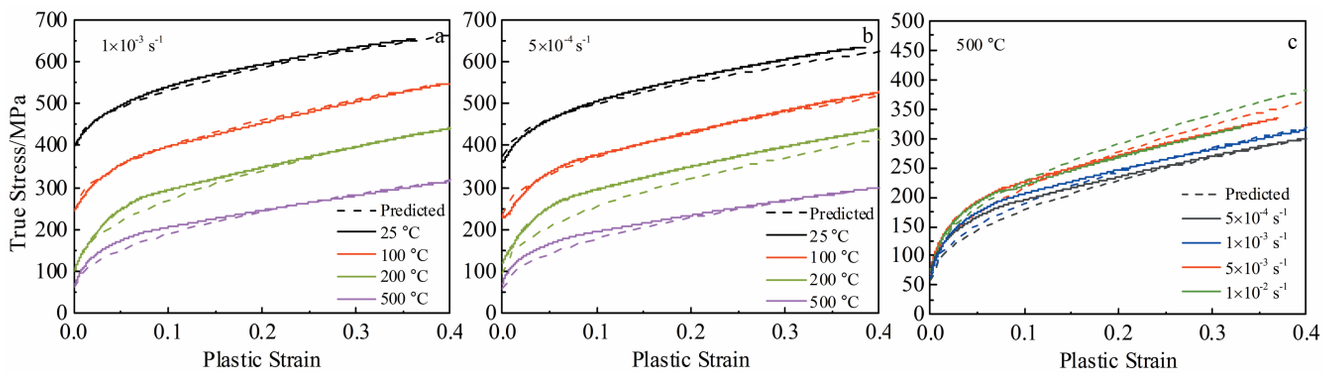

Fig.15 Comparison of model prediction results with tensile test curves: sampled data at $\dot{\varepsilon}$=1×10^{-3} s^{-1} (a), unsampled data at $\dot{\varepsilon}$=5×10^{-4} s^{-1} (b), and 500 ℃ (c)

It can be seen in Fig. 15c that the predicted error is relatively large at higher strain rates. This is because the parameters C in Eq. (2) is regarded as a constant, but in fact, it will change with the change of stress. In other words, $(\sigma_{0.2}/\sigma_{0.2r}-1)$ and $\ln\dot{\varepsilon}/\dot{\varepsilon}_0$ show a non-linear relationship. Therefore, the modified Johnson-Cook model cannot accurately capture the change of hardening behavior with strain rate.

3 Conclusions

1) The deformation resistance of pure molybdenum sheets decreases sharply at 25~300 ℃ and drops slowly with temperature at 300~500 ℃ due to the dynamic strain aging. Consequently, the flow stress is insensitive to strain rate at 300~500 ℃.

2) The strain hardening exponent increases from 0.15 at RT to about 0.3 at 300 ℃ and then varies little with increasing the temperature. A two-step hardening can be observed at all temperatures and strain rates. The second step shows a linear decrease in working hardening rate with the slope inversely proportional to the deformation temperature.

3) Recrystallization changes the texture strength without changing the texture type of the rolled sheet. After annealing, weakening of γ-fiber texture intensities reduces r value of molybdenum sheet. The normal anisotropy is not affected by temperature and strain rate.

4) The elongation to fracture increases with temperature, reaching a peak at about 200 ℃, and then decreases slightly. The drop in elongation to fracture results from the dynamic strain aging. Tensile specimen undergoes a mixed mode of intergranular fracture and transgranular fracture. The increase of temperature can suppress the generation of intergranular cracks and intragranular cracks, resulting in a decrease in the number of fracture layers as the temperature increases. Delamination of the fracture surface results from intergranular cracks which are induced by the additional tensile stress along ND after necking. The formation of intergranular cracks can retard the deformation localization in the necking region.

5) The constitutive relation of the molybdenum sheet can be predicted by a modified Johnson-Cook model, in which the quadratic function is adopted to depict the variation of key parameters with temperature. The average error of the model prediction is less than 5%.

References

1 Xiao M, Li F, Xie H *et al*. *Materials & Design*[J], 2012, 34: 112

2 Fu J B, Yang Q L, Zhuang F *et al*. *China Molybdenum Industry* [J], 2013(4): 40

3 Walde T. *International Journal of Refractory Metals & Hard Materials*[J], 2008, 26: 396

4 Zhang J X, Liu Y Q, Zhou M L *et al*. *Rare Metal Materials and*

Engineering[J], 2005, 34(2): 221 (in Chinese)
5 Niu R M, Zhang G J, Sun J *et al*. *Rare Metal Materials and Engineering*[J], 2006, 35(4): 559 (in Chinese)
6 Fan X G, Yang H, Gao P. *Chinese Science Bulletin*[J], 2014, 59: 2859
7 Fan X G, Zhang Y, Gao P F *et al*. *Materials Science and Engineering A*[J], 2017, 694: 24
8 Zhang Z Y, Yang H, Li H *et al*. *Materials Science and Engineering A*[J], 2013, 569: 96
9 Huang W, Zan X, Nie X *et al*. *Materials Science & Engineering A*[J], 2007, 443: 33
10 Kocks U F, Mecking H. *Progress in Materials Science*[J], 2003, 48: 171
11 Oertel C G, Huensche I, WSkrotzki *et al*. *Materials Science & Engineering A*[J], 2008, 483-484: 79
12 Kleiser G, Revil-Baudard B, Cazacu O *et al*. *JOM*[J], 2015, 67: 2635
13 Kleiser G, Revil-Baudard B, Cazacu O *et al*. *International Journal of Solids and Structures*[J], 2015, 75-76: 287
14 Juntunen P, Karjalainen P, Raabe D *et al*. *Metallurgical and Materials Transactions A*[J], 2001, 32: 1989
15 Johnson, Gordon R. *Proceedings of the 7th International Symposium on Ballistics*[J]. 1983, 21(1): 541
16 Lin Y C, Chen X M. *Materials & Design*[J], 2011, 32: 1733
17 Liang R, Khan A S. *International Journal of Plasticity*[J], 1999, 15(9): 963
18 El-Magd E, Abouridouane M. *International Journal of Impact Engineering*[J], 2006, 32: 741
19 Ulacia I, Salisbury C P, Hurtado I *et al*. *Journal of Materials Processing Technology*[J], 2011, 211: 830
20 Chen Y, Clausen A H, Hopperstad O S *et al*. *International Journal of Solids and Structures*[J], 2009, 46: 3825
21 Cheng Y Q, Zhang H, Chen Z H *et al*. *Journal of Materials Processing Technology*[J], 2008, 208: 29
22 Zhang H, Wen W, Cui H. *Materials Science and Engineering A* [J], 2009, 504: 99

纯钼薄板的温变形行为及本构建模

代　鹏[1]，高晗菲[2]，王　宁[2]，樊晓光[2]，孙明明[1]
(1. 兰州空间技术物理研究所 真空技术与物理重点实验室，甘肃 兰州 730000)
(2. 西北工业大学 凝固技术国家重点实验室，陕西 西安 710072)

摘　要：纯钼薄板在航天领域中有很好的应用前景，而准确表征纯钼板在温热条件下的力学性能是明确钼构件成形性的必要条件。因此，基于在不同温度（20~500 ℃）和应变速率（5×10^{-4}~1×10^{-2} s^{-1}）条件下进行的拉伸试验，对纯钼薄板的流动应力行为、厚向异性和断裂行为进行了研究。结果表明，纯钼薄板的变形抗力对温度敏感，同时，厚向异性指数r随温度变化较小。应变硬化指数从室温到300 ℃呈显著增大趋势，之后随着温度升高而趋于稳定。随着温度升高，纯钼薄板的断裂延伸率先升高后略减小。裂纹产生于晶界，随后晶粒沿着晶间裂纹的分离导致断口分层现象的产生。建立了修正的Johnson-Cook纯钼薄板本构模型，模型平均误差低于5%。

关键词：纯钼板；变形行为；厚向异性；断裂；本构模型

作者简介：代 鹏，男，1984年生，博士，兰州空间技术物理研究所，甘肃 兰州 730000，E-mail: daip2009@163.com